Studying Effects of Laser Penetration-Depth and Temperature on the Stability of Gabapentin-Loaded Au Nanoparticles

Zhenli Wei (lbozhang@gmail.com)
Zhejiang University Life Science Institute https://orcid.org/0000-0002-3607-1981
Reza Tayebee
Hakim Sabzevari University
Ehsan Koushki
Hakim Sabzevari University

Research Article

Keywords: gabapentin, drug delivery, Au NPs, CW laser beam, breast muscle of chicken, temperature effect

Posted Date: November 10th, 2021

DOI: https://doi.org/10.21203/rs.3.rs-1023595/v1

Studying effects of laser penetration-depth and temperature on the stability of gabapentin-loaded Au nanoparticles

Zhenli Wei[1,*], Reza Tayebee[2], Ehsan Koushki[3]

[1]*The Second Affiliated Hospital of Zhejiang University, School of Medicine, China*

[2]*Department of Chemistry, School of Sciences, Hakim Sabzevari University, Sabzevar, 96179-76487, Iran*

[3]*Department of Physics, School of Sciences, Hakim Sabzevari University, Sabzevar, 96179-76487, Iran*

Corresponding author: Zhenli Wei, Tel/Fax: +9844013212; lbozhang@gmail.com

Abstract

Herein, release of gabapentin molecules from gold nanoparticles (Au NPs) is studied by using two kinds of laser beams. The first is a green laser, which matches well with the frequency of the Au NPs' SPR and the second is a red laser that has the longest penetration depth in the tissue. Au NPs are synthesized by the Turkevich method and characterized with different techniques such as FT-IR, XRD, TEM, UV-VIS, and DLS. Then, the effects of two green and red lasers as well as temperature are investigated in the delivery of gabapentin drug molecules from Au NPs. Slices of chicken breast muscle with different thicknesses are also used in order to disclose an experimental condition close to the in vivo study. The drug release amount is, then, correlated with the return of the absorption-peak to its primary position. The effects of temperature and penetration depth of the laser beam investigated on the UV-VIS spectrum of Au NPs and the results are compared to attain the best release conditions. It is found that although the green laser is better than the red one to stimulate the SPR of Au NPs, however, the red laser is preferred for the drug delivery purposes due to its greater penetration depth. Also, increasing the temperature of the capped nanocolloid enhances the rate of drug release by the laser irradiation. Therefore, this investigation is helpful to understand the effect of temperature and a red laser beam on different metallic nanoparticles carrying drug molecules.

Keywords: gabapentin . drug delivery . Au NPs . CW laser beam . breast muscle of chicken . temperature effect

Introduction

Nanomaterial drug delivery is an emerging field that has significant advantages over conventional therapy and has been suggested as a powerful tool to improve the efficacy of chemotherapeutics with potential applications in diagnostic developments [1-2]. Therefore, nanoparticles have been extensively used in medicine research because of their unique properties such as high specific surface area, increased solubilization of hydrophobic drugs, tunable targeting properties, controlled drug release, effective permeability and penetration properties as well as easy modification [3-12].

Epilepsy is a serious neurological disorder associated with sporadic symptoms and abnormalities such as psychiatric disorders, cognitive impairment, and social problems. Gabapentin is an antiepileptic drug with no rmothymic properties that is used for the treatment of seizures and neuropathic pain. Unfortunately, oral bioavailability of the target drug alewiates with dose (42 and 60% under the administration of 600 and 300 mg, respectively) [13], therefore, formulation of gabapentin loaded nanovehicles may facilitate delivery of higher amounts of this drug towards more effective medication.

Au nanoparticles have shown more attention in drug delivery and have been increasingly applied in biomedical investigations due to their low toxicity, broad antimicrobial and visible light extinction behavior, sufficient stability under most physiological conditions, surface reactivity, and surface plasmon characteristics [14-17]. Au nanoparticles display a unique combination of chemical, physical, optical and electronic properties different from other biomedical nanovehicles and provide a wide multifunctional platform in drug delivery systems [18-19]. Owing to the relatively large size of Au NPs, they can be used to deliver drugs with low solubility and poor pharmacokinetic properties to the target tissues, control the drug release and frequency, increase bioavailability, and decrease side effects of the drug [20-22].

Now a days, many experiments are performed on the delivery of different drugs by using a wide range of biocompatible nanoparticles. Herein, it has been tried to load gabapentin onto the surface of citrate-capped Au nanoparticles in a colloidal solution prepared by the Turkevich method. The loading/releasing process is monitored by UV-VIS spectroscopy to record the blue/red shift in the absorption peak. Therefore, we try to match the laser light frequency with

the SPR frequency of Au NPs and control the loading/ release process. Thus, the two green and red lasers are used to push the release of gabapentin molecules from the surface of Au NPs and different behavior of red and green lasers is detected. The green laser matches well with the frequency of the SPR, whereas the red one has the longest penetration depth in the chicken tissue. Therefore, slices of the breast muscle of chicken with different thicknesses were used in order to assemble the real in vivo conditions. After that, the drug release amount was correlated with the return of absorption maximum to its primary position. The effects of temperature and penetration depth of the laser beam were also studied on the UV-VIS spectrum of Au NPs and compared to attain the best releasing conditions. To the best of our knowledge, it is the first report describing the influence of laser beam on an animal tissue by using the principles of Au NPs' SPR. Moreover, effect of temperature on the release of drug from Au NPs is studied for the first time.

Results and discussion

Characterization of Au NPS

Fig. 1 shows the FT-IR spectra of the surface modified Au NPs with citrate (Au@citrate, a) and surface modified Au NPs with both citrate and gabapentin (Au@citrate-gabapentin, b). The broad band at about 3200-3600 cm^{-1} in both spectra is related to the C-OH and H_2O stretching vibrations. Weak bands in 2850-2950 cm^{-1} in Au@citrate are due to CH_2 vibrations. The two peaks around 1385 and 1589 cm^{-1} in (a) are due to the symmetric and asymmetric stretching of CO_2^- in citrate. These characteristic peaks were also observed in the FT-IR of gabapentin drug loaded Au NPs decorated with citrate. In addition, new medium characteristic peaks due to gabapentin were also identified at 2928 cm^{-1} (NH_3^+), 2151 cm^{-1} (C-N), 1650-1540 cm^{-1} (asymmetric carboxylate and NH_3^+ deformation). It should be mentioned that gabapentin is a zwitterion in the solid state and there was no FT-IR band in the usual NH stretching region (3500-3300 cm^{-1}).(Chimatadara et al., 2007).

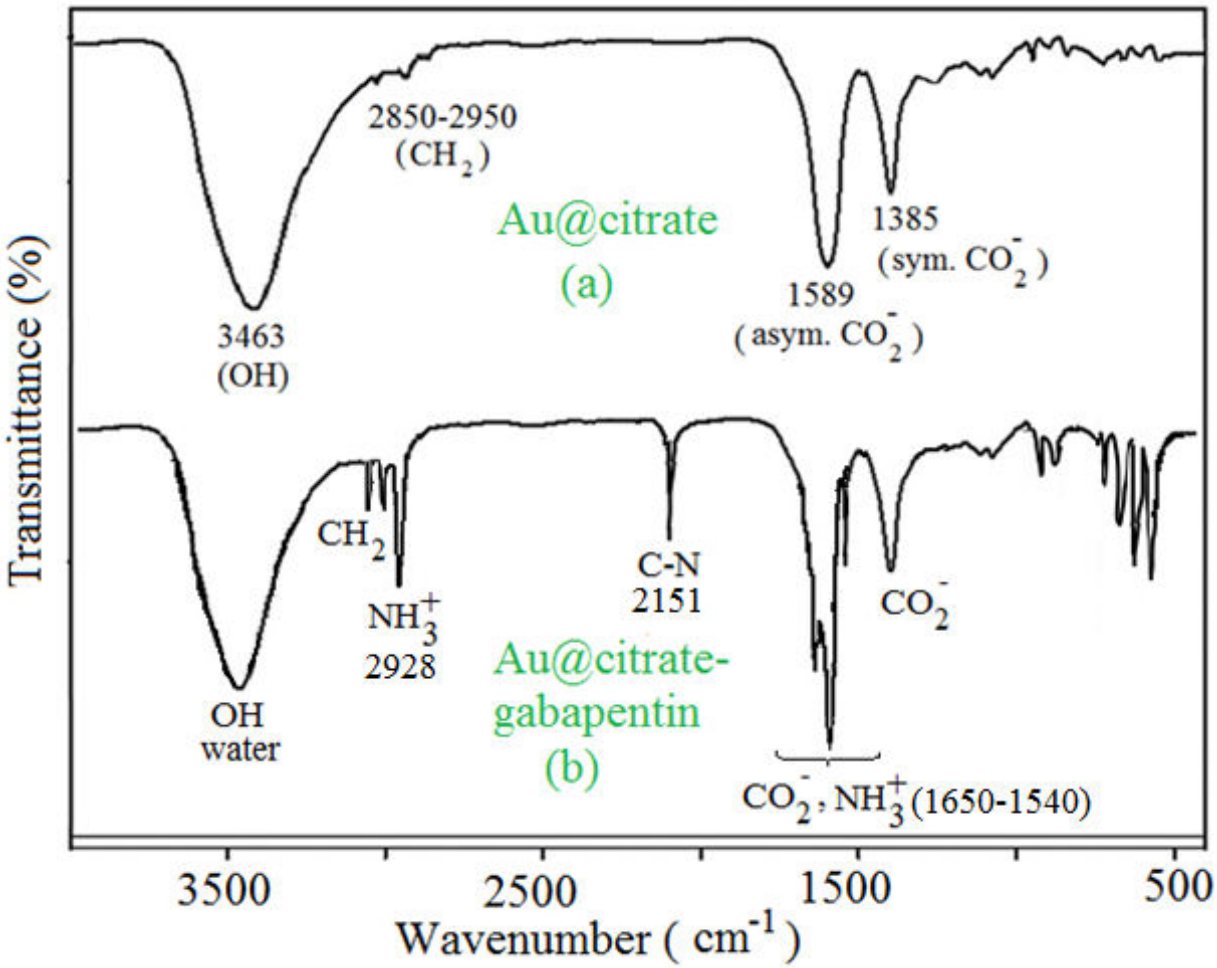

Fig. 1. FT-IR spectra of surface modified Au NPs with citrate (Au@citrate, a) and surface modified Au NPs with both citrate and gabapentin (Au@citrate-gabapentin, b).

The absorption spectrum of the aqueous drug solution and Au nanocolloid are compared as shown in Fig. 2. The drug has a medium peak at 230 nm that can be used to determine its concentration. The peak of absorption saddens at 530 nm is also due to SPR of Au NPs. The size distribution of Au NPs was assessed by DLS through calculating the hydrodynamic diameter of the particles. As shown in Fig. 3, the average hydrodynamic size is obtained about 24 nm. The XRD pattern of the synthesized Au NPs are shown in Fig. 4a that confirms formation of nanoparticles with a cubic structure. The remarkable peaks at the 2 theta 38.3, 44.5, 64.6, and 77.6° are devoted to the face-centered cubic gold with the 111, 200, 220 and 311 crystallographic planes, respectively, in accordance with the card number JCPDS No.04-0784 [21, 23]. Fig. 4b at the inset shows the TEM image of Au NPs that confirmed regular spherical particles with sized <

25 nm [24]. In Fig. 5, the absorption spectra of Au nanocolloids before and after drug loading are compared. As shown, although addition of a clear solution of the drug dilutes the final solution and reduces the height of the spectrum, however, the loading process caused the peak to experience a blue-shift.

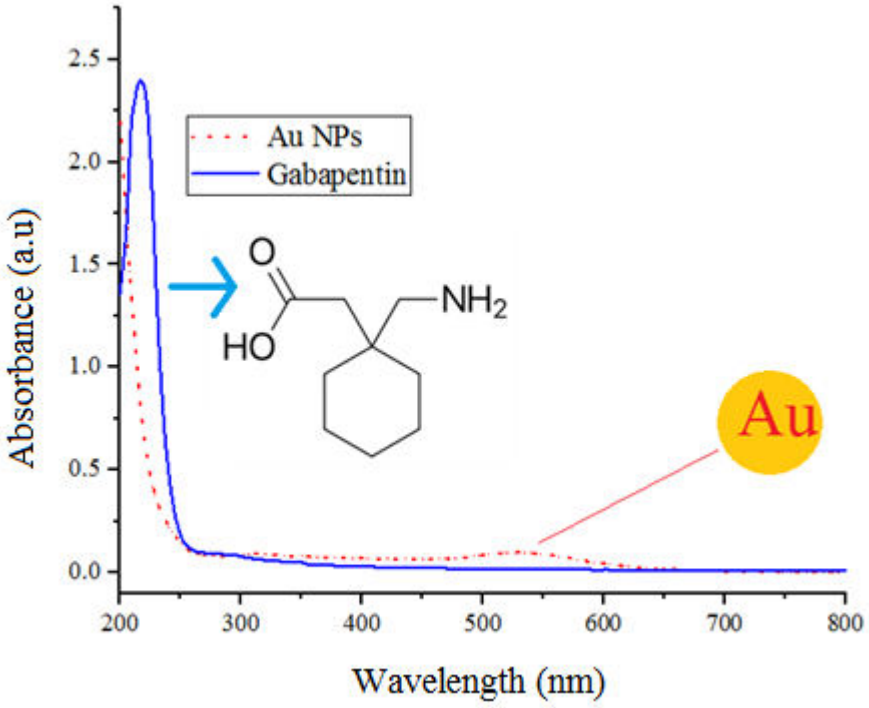

Fig. 2. UV-VIS spectra of gabapentin and the as-synthesized Au NPs.

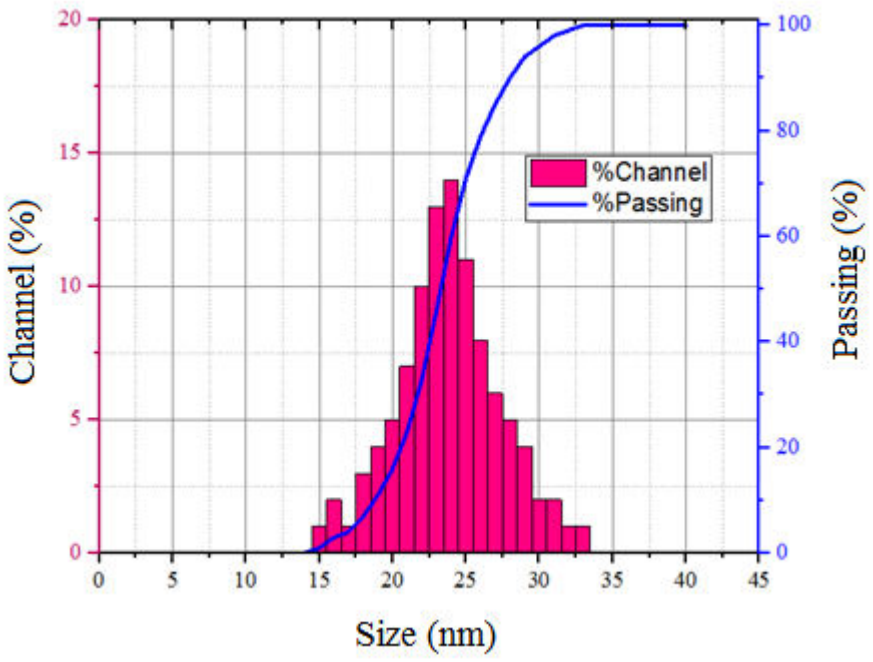

Fig. 3. Dynamic light scattering (DLS) measurement of the synthesized Au NPs.

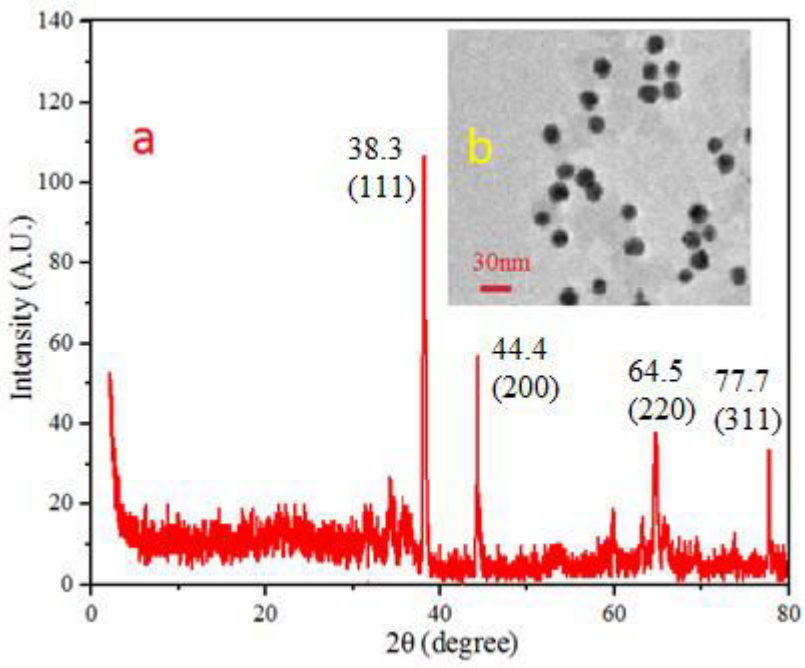

Fig. 4. The XRD diffraction pattern (a) and TEM image (b) of the as-synthesized gold nanoparticles.

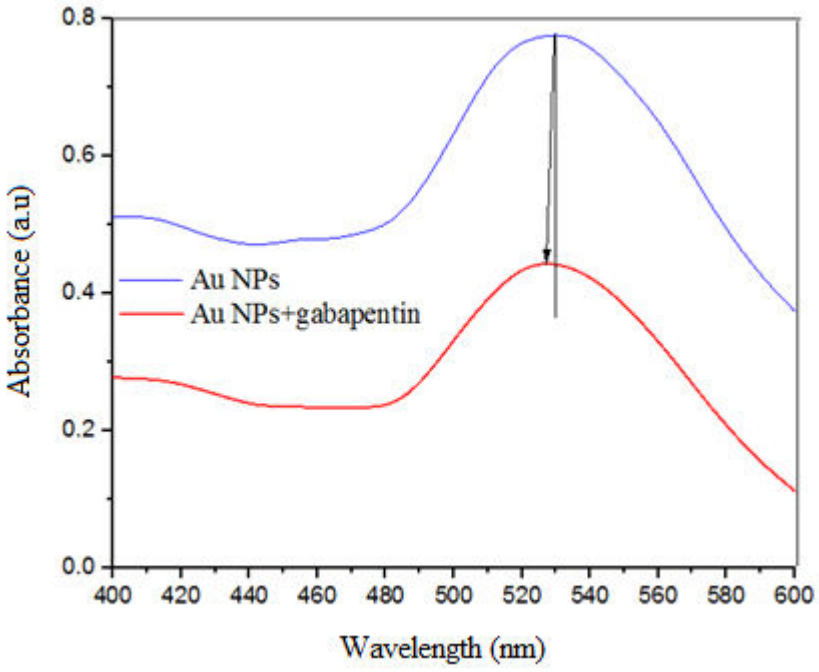

Fig. 5. Comparison of the UV-Visible spectra of the synthesized Au NPs before and after drug loading.

Effect of laser beam on the release of gabapentin

This study focused on the release of drug with two manners including irradiation of a laser beam towards the drug loaded nanoparticles and enhancing temperature of the colloidal solution. The two lasers were selected to start the drug release. The green laser has the most wavelength matching well with the SPR of Au NPs and a red laser, which has the longest depth of penetration in the chicken tissue. When the two lasers with the same output power (2 mW) were emitted toward the drug-loaded nanocolloids, the peak of absorption (λ_{max}) was returned to its initial value, which indicated the release of the drug from nanoparticles. Fig. 6 shows the blue shift of λ_{max} as the laser beam is incident to the colloid. As shown in this Figure, the green laser beam can force the release process further, which was in good agreement with the previous reports [25].

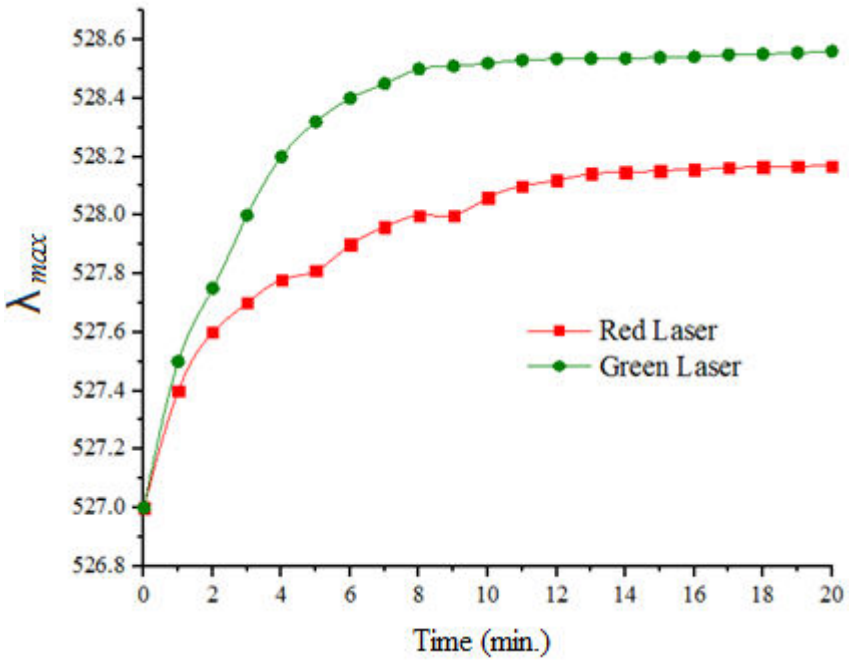

Fig. 6. Shift of the surface plasmon resonance (SPR, nm) *vs* time of the laser illumination.

It is noticeable that Au NPs can absorb the laser irradiation and generate a small amount of heat. Absorption of the green laser beam was higher and created more heat. Heating Au NPs may increase the kinetic energy of the surface electrons and affect the release process. However, the created heat is not sufficient to change the structure of drug molecules. Furthermore, the thermal effects related to the continuous wave (CW) lasers are insignificant and increasing of temperature would not be greater than 1 °C in the solution [26].

In the next step, we studied the depth of penetration of the laser beam in the tissue to simulate the in vivo conditions. We used slices of chicken breast muscle with different thicknesses. As the experimental setup at Fig. 7 shows, the laser beam with the same output intensity were transmitted from the slices and the transmitted powers were recorded *vs* the muscle thickness, as shown in Fig.8. By numerical fitting of these curves with the Bear-Lambert law ($I = I_0 \exp(-\alpha L)$), the absorption coefficient of the chicken breast muscle was obtained $\alpha = 0.22\ {}^{1}\!/_{cm}$ for the red light and $\alpha = 0.26\ {}^{1}\!/_{cm}$ for the green one.

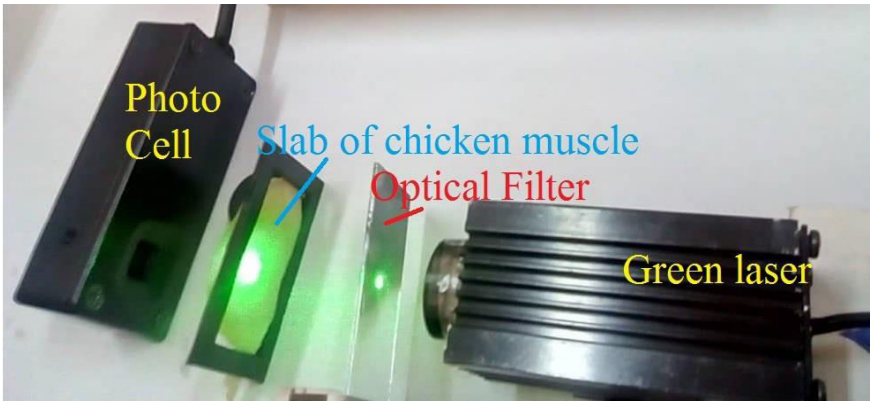

Fig. 7. The experimental measurement of the optical transmittance through a slab of the chicken breast muscle.

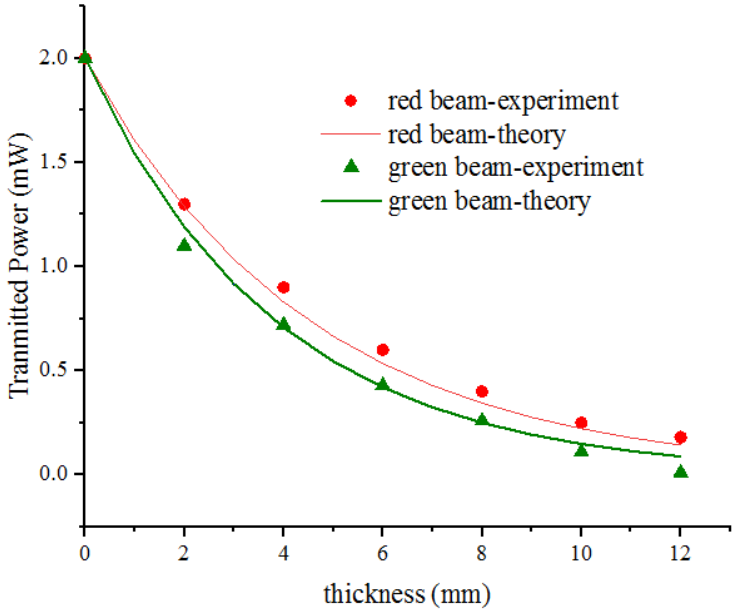

Fig. 8.The experimental results of the penetration depth by using the laser beam to achieve the absorption coefficient.

In Fig. 9, the beams were incident to the gabapentin nanocolloid after passing through the slabs with the thickness of *d*. As shown, by increasing *d*, the rate of drug release was decreased and saddened for the two laser beams. Also, for thin layers of slabs, the green laser was more efficient for the release process because of its well matching with the frequency of Au NPs' SPR. By enhancing *d*, the rate of release was decreased suddenly for the green laser, but this change

was less pronounced for the red laser and the tissue affected less on it; thus, more penetration depth of the red laser.

Considering the laser's wavelength, it should have a low penetration depth in the tissue. Thus, we achieved a low intensity laser to limit the uncontrolled and unknown side effects such as reshaping, warming and degradation of the drug loaded NPs. The penetration-depth of the applied light depends directly to the wavelength. Generally, the penetration depth of the light depends to its wavelength. For example, the blue light has a short penetration depth (< 3 mm) and can be absorbed by the skin epidermis. Whereas, the penetration-depth of a green light is ~5 mm and may reach to the dermis layer of skin. But, the red beams can penetrate some centimeters and reach the blood vessels [27-28]. The above penetration depth can be slightly altered by increasing the irradiation intensity. Therefore, a red laser can be helpful for the in-vivo purposes.

In the next step, we studied effect of temperature on the efficiency of release process by using the laser beam. In Fig. 10, the laser beam is directly incident to the colloid and the shift of λ_{max} is plotted *vs* time. This experiment was repeated at different temperatures (30-40°C). As shown, by absorbing light with the nanoparticles at a higher temperature, the energy of the gabapentin molecules to get rid of the particles was increased and the release process became more accessible. This result is in good agreement with the previous report [29], which shows the release of DNA molecules from Au NPs is temperature-dependent.

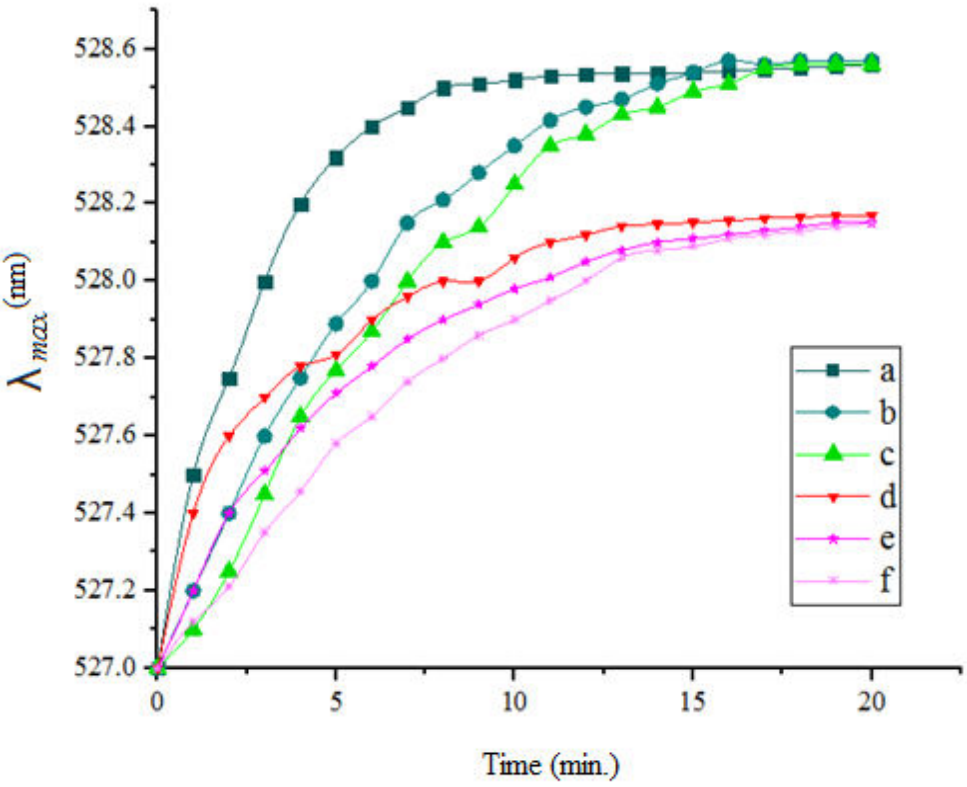

Fig. 9.Shift of the surface plasmon resonance (SPR, nm) *vs* time of laser illumination after passing through the slab with the thickness of *d*: (a) green laser, *d*=0; (b) green laser, *d*=5mm; (c) green laser, *d*=10mm; (d) red laser, *d*=0; (e) red laser, *d*=5mm; (f) red laser, *d*=10mm.

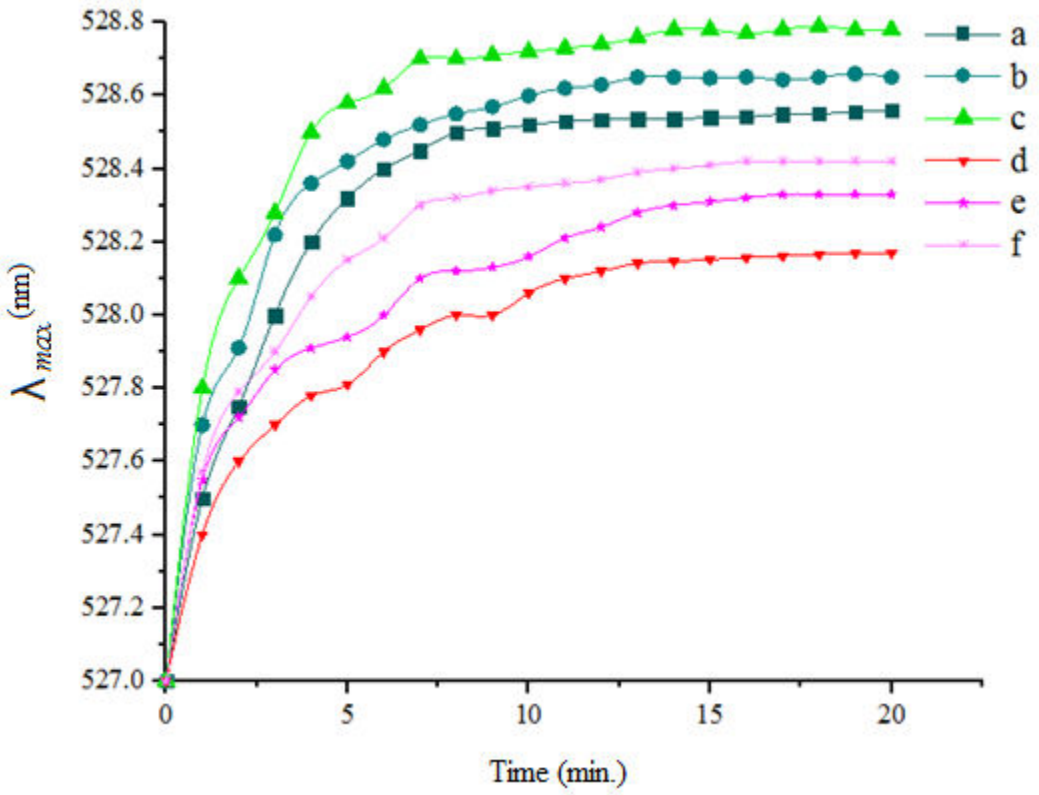

Fig. 10. Shift of the surface plasmon resonance (SPR, nm) vs time of laser illumination at different temperatures. (a) green laser, t=40°C;(b) green laser, t=35 °C;(c) green laser, t=30 °C; (d) red laser, t=40 °C; (e) red laser, t=35 °C; (f) red laser, t=30 °C.

At final, it is necessary to review different mechanisms of drug loading onto the surface of Au NPs. Detailed mechanistic studies are required to disclose the mechanism of drug adsorption on the surface of Au NPs, however, three possible mechanisms are known in this process. They are hydrogen bonding interaction, hydrophobic interaction, and Lewis acid-base interaction. The first interaction that is not so strong describes adsorption of drug molecules through hydrophobic functional groups. Hydrogen bond interaction mainly occurs in the adsorption of polar drug molecules and occurs via the lone-pair hydrogen bonding donors of drug molecules with the acceptor sites on the surface of NPs. The latter Lewis acid-base interaction commonly happens through the polar groups of drug molecules. Therefore, the above mentioned interactions can be regarded as the electronic interactions between the drug molecule

and surface of an adsorbent. In addition, citrate displacement with gabapentin is another route, which can be accounted for the interaction of drug molecules with Au NPs decorated with citrate ions, as all of these options are shown in Fig.11.

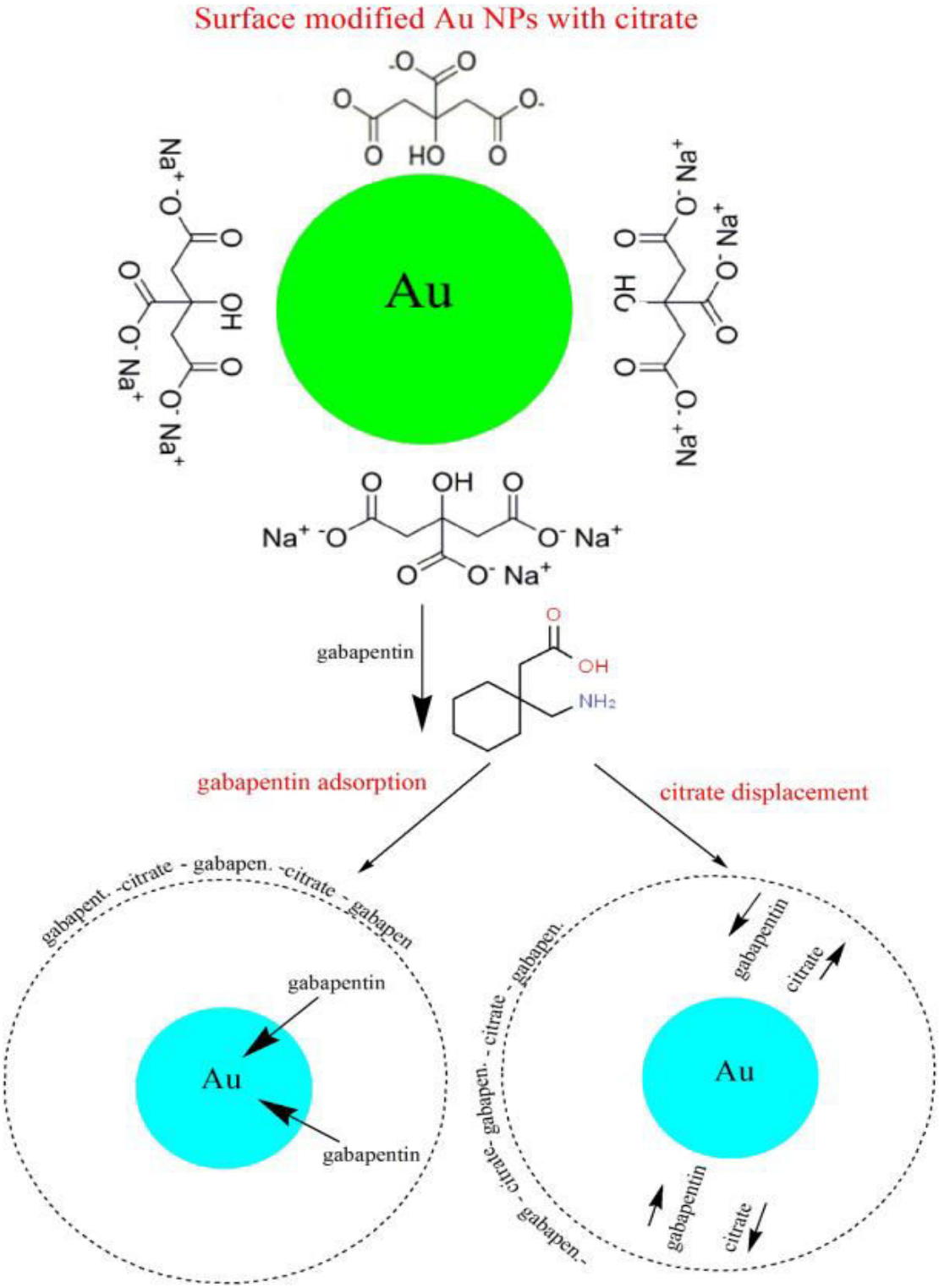

Fig.11. A schematic representaion for the plausible interactions of citrate and cetirizine with Au nanoparticles.

Conclusion

In summary, effects of temperature and penetration depth of green and red lasers are studied in the delivery of gabapentin drug molecules from Au NPs. These nanoparticles are synthesized by the Turkevich reduction method and characterized with different techniques including XRD, TEM, UV-VIS, and DLS. Gabapentin molecules are loaded onto the surface of Au NPs, as confirmed by a blue-shift in the absorption spectrum. To release the gabapentin molecules from the surface of Au NPs, two laser beams are used; green and red. Slices of chicken breast muscle with different thicknesses are performed in order to study the penetration depth of the laser beam. The effects of temperature and penetration depth of the laser beam are studied on the absorption spectrum of Au NPs and the results are compared to attain the best release conditions. It is found that although the green laser is better than the red one to stimulate the SPR of Au NPs, however, the red laser is preferred for the drug delivery purposes due to its greater penetration depth. Also, enhancing the temperature of Au NPs decorated with gabapentin can enhance the rate of release by the laser irradiation. Thus, this study is beneficial to found effect of temperature and laser irradiation on various metal-based NPs bearing drug molecules.

Experimental

Materials and methods

All of the primary materials were attained from commercial resources and used with no excess purification. Tetrachloroauric acid monohydrate ($HAuCl_4 \cdot H_2O$), trisodium citrate dihydrate and gabapentin were purchased from Sinopharm Ltd (Beijing, China) with high purity (99.9 % assay). The XRD analysis was performed on a PW1800- Phillips diffractometer with Cu Kα radiation (λ= 1.5418 Å) at 40 keV and 40 mA to attain the crystal structure of the fabricated Au NPs. Ultraviolet-visible spectra were achieved on a UV-VIS Array Spectrophotometer (detection limit 0.1 nm). Particle size and distribution of the nanoparticles were assessed by dynamic light scattering (DLS) on a Malvern Zetasizer 3000. Transmission electron microscopy (TEM) was done on a Philips CM120 with the magnification of 200 K.

Synthesis of Au NPs

To synthesize Au NPs, 60 mg of sodium citrate was added to6 mL distilled water and stirred at 100 ℃ for 10 min. 2 mL of $HAuCl_4$ solution (1 wt%) was added to20 mL distilled water and warmed up to boiling. Thereafter, the sodium citrate solution was added to the tetrachloroauric acid monohydrate solution and put on a hotplate for 5 min at 100 $^{\circ}$C, then cooled to room temperature. The ruby red color of the cooled colloid indicated formation of Au NPs.

Decoration of Au NPs with gabapentin

The drug was loaded onto Au NPs as follows. 2 mL of gabapentin solution with a concentration of 2.5 g/L was prepared in deionized water. This solution was then added to 8 mL of the prepared AuNPs colloidal solution and the resulting mixture was incubated at room temperature for 12 h and followed by sonication for 10s. Finally, the attained solution was stored at room temperature.

Calculation of loading/ release of the drug

The drug-loading capacity (Eq.1) was calculated by differentiating the free drug remained in the solution after delivery from the total amount of the primary drug. The amount of unloaded gabapentin was simply determined by UV-VIS spectrophotometry at 230 nm against a blank. Therefore, the loading capacity can be calculated from Eq. 1.

$$\text{Loading capacity } (\%) = M_0 - M_t / M_N \times 100 \qquad \text{Eq. (1)}$$

where M_0 and M_t are the drug amount in the primary and final solutions, respectively. M_N is the amount of the used Au NPs. In this experiment, the medium loading capacity of 65% was obtained after triplicate experiments.

Funding Information:

The work has been was supported by Hakim Sabzevari university.

Compliance with Ethical Standards

Conflict of interest: The authors have no competing interests to declare that are relevant to the content of this article.

Consent to publish: The authors affirm that human research participants provided informed consent for publication of this article.

Consent to Participate: Informed consent was obtained from all individual participants included in the study.

Ethical approval: Ethical approval was waived by the local Ethics Committee of Hakim Sabzevari University in view of the retrospective nature of the study and all the procedures being performed were part of the routine care.

Availability of data and material

All data generated or analyzed during this study are included in this published article.

Code availability

Not applicable

Author contributions:

Z. W.-conceptualization, formal analysis; E.K.- methodology, writing original draft, processing of results; R.T.- visualization, writing original draft, editing.

References

1. Crous A, Abrahamse H. Innovations in Nanotechnology for Biomedical Sensing, Imaging, Drug Delivery, and Therapy. Nanotoxicology. 2021 Jul 14:21-42.

2. Yadav HK, Usman S, Ghanem KA, Beevi R. Synthesis of Nanomaterials for Drug Delivery. In Functionalized Nanomaterials II 2021 Apr 11 (pp. 23-44). CRC Press.

3. Saravanan S, Nangai EK, Ajantha SV, Sankar S. Recent Developments in Nanomaterial Applications. In Nanomaterials and Nanocomposites 2021 Apr 5 (pp. 3-15). CRC Press.

4. Krishnan S, Joseph B, James J, Thomas S. Nanomaterials for Cancer Therapeutics. InNanoparticles for Drug Delivery 2021 (pp. 1-20). Springer, Singapore.

5. Mir MA, Bhat BA, Sheikh BA, Rather GA, Mehraj S, Mir WR. Nanomedicine in Human Health Therapeutics and Drug Delivery: Nanobiotechnology and Nanobiomedicine. In Applications of Nanomaterials in Agriculture, Food Science, and Medicine 2021 (pp. 229-251). IGI Global.

6. Tayebee R, Fattahi Abdizadeh M, Mohammadpour Amini M, Mollania N, Jalili Z, Akbarzadeh H. Fe_3O_4@SiO_2-NH_2 as an efficient nanomagnetic carrier for controlled loading and release of acyclovir. International Journal of Nano Dimension. 2017 Oct 1; 8(4):365-72.

7. Xie X, Zhang L, Zhang W, Tayebee R, Hoseininasr A, Vatanpour HH, Behjati Z, Li S, Nasrabadi M, Liu L. Fabrication of temperature and pH sensitive decorated magnetic nanoparticles as effective biosensors for targeted delivery of acyclovir anti-cancer drug. Journal of Molecular Liquids. 2020 Jul 1; 309:113024.

8. Akbarzadeh H, Tayebee R. Adsorption mechanism of different acyclovir concentrations on 1–2 nm sized magnetite nanoparticles: A molecular dynamics study. Journal of molecular liquids. 2018 Mar 15; 254: 64-9.

9. Dou X, Keywanlu M, Tayebee R, Mahdavi B. Simulation of adsorption and release of doxepin onto ZIF-8 including in vitro cellular toxicity and viability. Journal of Molecular Liquids. 2021 May 1; 329:115557.

10. Fu M, Tayebee R, Saberi S, Nourbakhsh N, Esmaeili E, Maleki B, Vatanpour HR. Studying Adsorption and Cellular Toxicity of Boron Nitride Nanostructure versus Melphalan Anti-ovarian Cancer Drug. Current Molecular Medicine. 2021.

11. Hoseininasr AS, Tayebee R. Synthesis and characterization of superparamagnetic nanohybrid Fe_3O_4/NH_2-Ag as an effective carrier for the delivery of acyclovir. Applied Organometallic Chemistry. 2018 Dec; 32(12):e4565.

12. Guo R, Liu Q, Wang W, Tayebee R, Mollania F. Boron nitride nanostructures as effective adsorbents for melphalan anti-ovarian cancer drug. Preliminary MTT assay and in vitro cellular toxicity. Journal of Molecular Liquids. 2021 Mar 1; 325:114798.

13. Gaur PK, Mishra S, Kumar A, Panda BP. Development and optimization of gastro retentive mucoadhesive microspheres of gabapentin by Box–Behnken design. Artificial cells, nanomedicine, and biotechnology. 2014 Jun 1; 42(3):167-77.

14. Asadishad B, Vossoughi M, Alamzadeh I. In vitro release behavior and cytotoxicity of doxorubicin-loaded gold nanoparticles in cancerous cells. Biotechnology letters. 2010 May; 32(5):649-54.

15. Kasthuri J, Veerapandian S, Rajendiran N. Biological synthesis of silver and gold nanoparticles using apiin as reducing agent. Colloids and Surfaces B: Biointerfaces. 2009 Jan 1;68(1):55-60.

16. Singh P, Pandit S, Mokkapati VR, Garg A, Ravikumar V, Mijakovic I. Gold nanoparticles in diagnostics and therapeutics for human cancer. International journal of molecular sciences. 2018 Jul; 19(7):1979.

17. Liu XY, Wang JQ, Ashby Jr CR, Zeng L, Fan YF, Chen ZS. Gold nanoparticles: synthesis, physiochemical properties and therapeutic applications in cancer. Drug discovery today. 2021 Feb 4.

18. Chen J, Glaus C, Laforest R, Zhang Q, Yang M, Gidding M, Welch MJ, Xia Y. Gold nanocages as photothermal transducers for cancer treatment. Small. 2010 Apr 9; 6(7):811-7.

19. Von Maltzahn G, Park JH, Agrawal A, Bandaru NK, Das SK, Sailor MJ, Bhatia SN. Computationally guided photothermal tumor therapy using long-circulating gold nanorod antennas. Cancer research. 2009 May 1; 69(9):3892-900.

20. Lone MN, Wani IA, Yatoo GN, Zubaid U, Banday JA. Role of Gold Nanoparticles in Drug Delivery and Cancer Therapy. InApplications of Nanomaterials in Agriculture, Food Science, and Medicine 2021 (pp. 124-140). IGI Global.

21. Liu Y, Chen F, Wang Q, Wang J, Wang J, Guo L, Gebremariam TT. Plasmonic-enhanced catalytic activity of methanol oxidation on Au–graphene–Cu nanosandwiches. Nanoscale. 2019; 11(18):8812-24.

22. Lopes CM, Bettencourt C, Rossi A, Buttini F, Barata P. Overview on gastroretentive drug delivery systems for improving drug bioavailability. International journal of pharmaceutics. 2016 Aug 20; 510(1):144-58.

23. Jiang Z, Zhang Q, Zong C, Liu BJ, Ren B, Xie Z, Zheng L. Cu–Au alloy nanotubes with five-fold twinned structure and their application in surface-enhanced Raman scattering. Journal of Materials Chemistry. 2012; 22(35):18192-7.

24. Koushki E. Effect of conjugation with organic molecules on the surface plasmon resonance of gold nanoparticles and application in optical biosensing. RSC Advances. 2021; 11(38):23390-9.

25. Yan S, Li Q, Nie H, Wang S. Studying delivery of neuroprotective gabapentin drug by gold nanoparticles using a laser beam affecting surface plasmon resonance. Chemical Papers. 2021 Jul 23:1-7.

26. Koushki E, Farzaneh A. Time dependence of thermo-optical effect for thin samples containing light-absorptive material. Optics Communications. 2012 Mar 15; 285(6):1390-3.

27. Ruggiero E, Alonso-de Castro S, Habtemariam A, Salassa L. Up converting nanoparticles for the near infrared photoactivation of transition metal complexes: new opportunities and challenges in medicinal inorganic photochemistry. Dalton Transactions. 2016; 45(33):13012-20.

28. Chen G, Cao Y, Tang Y, Yang X, Liu Y, Huang D, Zhang Y, Li C, Wang Q. Advanced Near-Infrared Light for Monitoring and Modulating the Spatiotemporal Dynamics of Cell Functions in Living Systems. Advanced Science. 2020 Apr; 7(8):1903783.

29. Li F, Zhang H, Dever B, Li XF, Le XC. Thermal stability of DNA functionalized gold nanoparticles. Bioconjugate chemistry. 2013 Nov 20;24(11):1790-7.